DYNAMIC PROCESSES IN LIQUIDS AND GASES VISUALIZATION USING OF LASER REFRACTOGRAPHY TECHNIQUE

B.S. RINKEVICHYUS[C] , I.L. RASKOVSKAYA, A.V. TOLKACHEV

Department of Physics named V.A. Fabrikant, National Research University (MPEI), Moscow, 111250, Russia

[c]Corresponding author: Tel.: +74953627755; Fax: +74953628938; Email: rinkevbs@mail.ru

KEYWORDS:

    Main subjects: heat and mass transfer, flow visualization
    Fluid: liquids flows, boundary layers, two layers flows
    Visualization method(s): laser refractography
    Other keywords: digital image processing, structured laser beams

ABSTRACT: For visualizing non-stationary physical processes in liquids and gases, which arise when the gradient fields of temperature, pressure, density, salinity and others are in presence a new refractive method for flow investigation - Laser Refractography is used. On basis of structured laser beams the possibility of formation of exploratory area, which is a family of surfaces such as cylindrical, conical, or other type is carried out. Digital recording and processing of refraction patterns make it possible to simultaneously explore spatial and dynamic, including waves, characteristics of the physical processes in the liquid.

The objects of study are non-stationary temperature fields in the boundary layer, two-layer stratified salty fluid and wave processes in them, etc. The results of computer modeling and experimental diagnostics of the investigated processes are presented. Feature of the proposed algorithms for processing of the visualization results is the use of rigorous analytical and asymptotic methods to minimize the computational resources and in some cases to process the experimental results in real time.

INTRODUCTION. Optical methods for aerohydrodynamic flows investigations are one of the oldest methods [1-4], without which modern progress in the science and techniques would not be possible. Methods of flow diagnostics are based on the refraction of light beams on the large-scale optical inhomogeneities. In these devices different space filters (Zernike, Hilbert, Fuco), placed in the focal plane, are used.

Expensive high-quality optical elements and optical processing of images are used in schlieren devices. They are bulky, difficult in adjustment and exploitation. That is why they are commonly used only in aerodynamic investigations of supersonic flows in industrial wind [2]. In investigations of physical processes in liquids schlieren devices are rarely used.

1. LASER REFRACTOGRAPHY TECHNIQUE

The usage of lasers together with Difractive Optical Elements (DOE) allows obtain spatially modulated laser beams of complicated structure. DOE represent thin plates with special phase patterns. When laser beam diffracts on such an element, the resulting beam becomes spatially modulated. That beam has got the name of Structured Laser Beam (SLB).

The initial laser beam possesses axial symmetry. By means of DOE, which is equal to linear diffraction screen, such a beam transforms into a number of divergent beams, placed in one plane. By means of DOE, which is equal to cylindrical lens, the laser beam is transformed into a divergent Laser Sheet (LS), linear in cross-section. A combination of cylindrical lens and diffraction grid allows to obtain up to 100 such lines.

The usage of DOE with more complicated phase pattern allows to obtain SLB with different structure: plane laser beam (laser sheet), plane laser beams, cross-shaped beams placed in orthogonal planes; conical beam; conical beams aggregate and etc. (Table 1).

The usage of the SLB gives the new possibility for laser refraction methods development. In [4] was considered the base principles of Laser Refractography (LAREF) – the diagnostics and visualizations technology of the boundary thin layered heterogeneities and edge effects in liquids, gas and plasma. This technology is based on the phenomenon of the structured SLB refraction in transparent heterogeneities [5], digital registration and computer processing of the refraction pictures [6]. Laser refraction methods possess the maximum obviousness and the ability of comparison of the computational and experimental refractograms because the measured quantity in those is the laser beam elements deflection magnitudes.

Table 1. Main types of SLB obtained with DOEs

Dot	12 by 5 Matrix	Line	Cross	Ring
•				

A schematic diagram of the LAREF technique is presented in Fig. 1. The radiation of laser *1* is transformed by optical system *2* into structured laser radiation that passes through scanning system *3* and then trough optically inhomogeneous flows *4* of interest – a liquid containing heated or cooled bodies – to form a 2D refractogram on semitransparent screen *5*.

The image of the 2D refractogram is recorded by digital camera *6* and entered in digital form into personal computer *7*, where it is processed by means of a special-purpose program. The processing of the refractogram allows one to qualitatively diagnose the gradient inhomogeneity in the liquids that caused the laser beams to refract; i.e., it allows obtaining information about temperature or concentration distribution 8 in the flow under study. Illustrated in the bottom row of the figure are the stages of formation of the refractogram from a narrow laser beam and also the plot obtained for the temperature dependence in a boundary layer next to a cooled ball immersed in hot water.
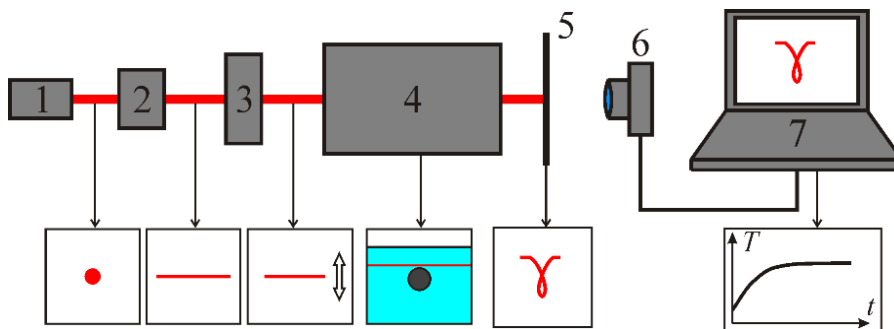.

Fig.1. Schematic diagram of the LAREF technique: *1* – laser, *2* – optical system,
3 – scanning system, *4* – medium under study, *5*– diffuse screen, *6* – CCD camera,
7 – personal computer, *8* – temperature distribution plot.

2. COMPUTER MODELLING OF DYNAMIC REFRACTOGRAMS

2.1. Laser beam propagation in dynamic plane layered medium

Let's review the propagation of laser beam along the Oz axis in inhomogeneous medium, consisting of three parts (Fig.2) [4]. The first part $(0 - z_1)$ – optically homogeneous medium with refractive index n_0. The second part $(z_1 - z_2)$ – optically inhomogeneous and dynamically medium with refractive index $n(y,t)$, depending on y and t, at that $n(z_2) = n_0$; the third part $(z_2 - z_3)$ – optically homogeneous medium with refractive index n_0. If the laser beam falls normally on such a medium, then in the first part it will propagate straightforward along the Oz axis. In the second part the beam will deviate toward the positive refractive index gradient. In the third part – the beam will propagate straightforward at the angle $\alpha_1(t)$ to the Oz axis.
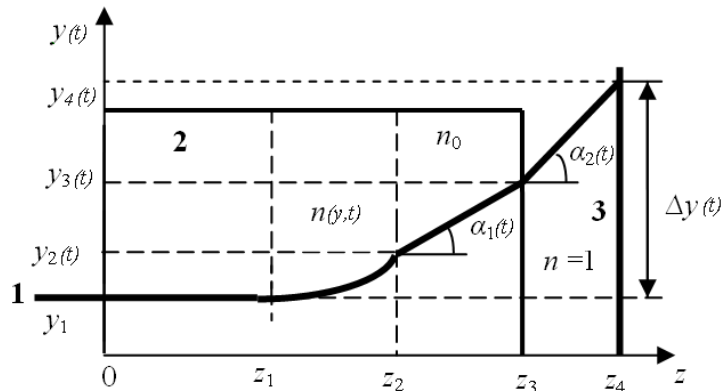
Fig. 2 Laser beam propagation in dynamic plane layer medium:
1 – laser beam, 2– investigated medium, 3 – screen

In LAREF technique the laser beam image shift is measured and it can easily be determined by geometry optics approach on the basis of ray propagation laws [7] or by beam optics approach, or the basis of wave propagation laws [8].

The angle of beam shift at the exit point of the second part of the media in the direction of y – axis α_1 is described by the equation

$$n(y_2,t)\sin[\alpha_1(y_2,t)] = n_0 , \qquad (1)$$

where $n(y_2,t)$ – refractive index in point y_2 at time t.

The exit point y_2 of the second part of the media can be obtained from the integral equation

$$z_2 = z_1 + n_0 \int_{y_1}^{y_2} [\sqrt{n^2(y) - n_0^2}]^{-1}dy. \qquad (2)$$

The exit angle at the second part of the medium is

$$\alpha_1(t) = \arcsin[n(y_2, t)n_0^{-1}], \qquad (3)$$

Full laser beam shift in the registration plane is

$$\Delta y(t) = y_2(t) - y_1 + [z_3 - z_2]\tan\alpha_1(t) + (z_4 - z_3)\tan\alpha_2(t). \qquad (4)$$

The form of the function $n(y,t)$ is determined by the properties of liquid and the refractive index distribution in the boundary layer. It should be mentioned, that expressions (1) and (2) do not contain restrictions for the refractive index gradient magnitude.
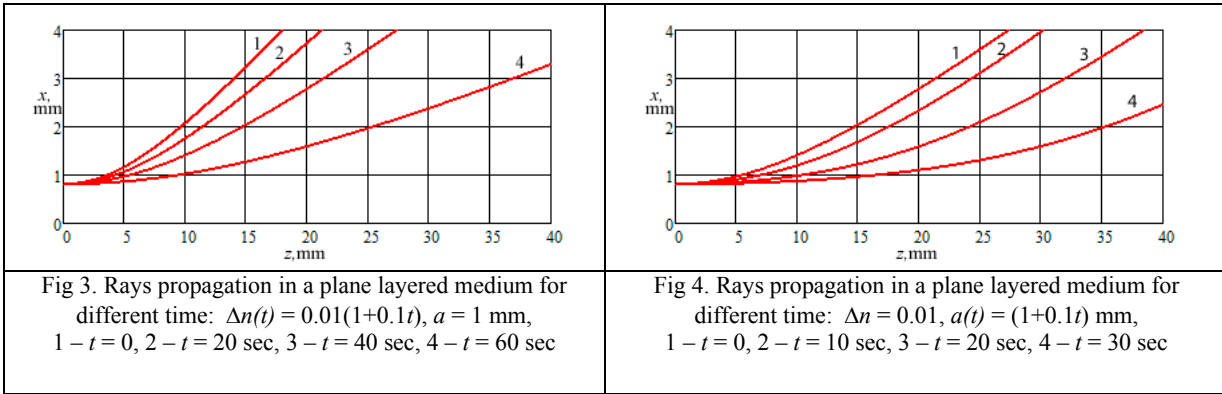
If we know, the law of refractive index variation, then the equation (2) gives the opportunity to calculate the trajectory of the beams in optically inhomogeneous medium. Expressions (1-4) allow calculate laser beam shift in the screen plane, which can be easily determined experimentally.

It is clear, that for rebuilding $n(y,t)$ only the measurement of the laser beam shift is insufficient. In order to make LAREF technique a quantitive one, it is supposed to compare two refractograms: the first one – calculated according to (2) and the second one – obtained by experiment. For calculation the refractogram it is necessary to carry out the calculation of the refractive index distribution in the investigation area by means of computation software and to use the medium refractive index dependence on temperature. For example for water at wavelength $\lambda = 0.6328$ μm the following refractive exponent dependence on temperature can be used $n(T)=1.33328 – 0.000051T – 0.0000011T^2$. Temperature T is measured in ^{o}C.

For exposure of beam propagation basic physical rules, let's consider exponential refractive index dependence on coordinate with time dependent parameters:

$$n(y,t) = n_0\{1 + \Delta n(t)\exp[-y/a(t)]\}, \qquad (5)$$

where $a(t)$ – typical width of temperature inhomogeneous layer near the heated body, $\Delta n(t)$ – maximum refractive index change. In the Fig. 2 trajectories of rayes passing on different distances from the surface are shown.

Fig 3. Rays propagation in a plane layered medium for different time: $\Delta n(t) = 0.01(1+0.1t)$, $a = 1$ mm, $1 - t = 0$, $2 - t = 20$ sec, $3 - t = 40$ sec, $4 - t = 60$ sec	Fig 4. Rays propagation in a plane layered medium for different time: $\Delta n = 0.01$, $a(t) = (1+0.1t)$ mm, $1 - t = 0$, $2 - t = 10$ sec, $3 - t = 20$ sec, $4 - t = 30$ sec

2.2 Laser beams propagation in dynamic spherical layered medium

Now we consider laser beam propagation in a spherical layered medium [4,7].

The LS refraction in spherical coordinates system (r,θ,φ) describes by followed equations which valid before or after turning point (indexed t) respectively (see Fig.5). The values at media input indexed by 0.
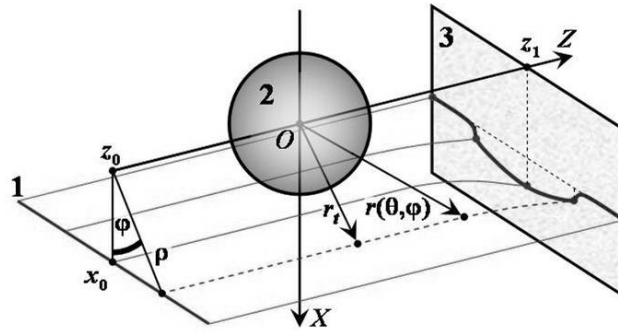

Fig. 5. The laser sheet refraction in dynamic spherically inhomogeneous medium:
1 – laser sheet, 2 – ball, 3 – screen

The coordinate of the ray returning point r_t may be find from equation $r_t n(r_t) = n_0 \rho_0$ and corresponding angle θ_t is

$$\theta(r,\phi,t) = \theta_0(\phi) + \int_{r_0(\phi)}^{r} \frac{n_0 x_0 \, dr}{r\cos\phi \sqrt{n^2(r,t)r^2 - n_0^2 \dfrac{x_0^2}{\cos^2\phi}}}, \tag{6}$$

the ray equation after the point of returning:

$$\theta(r,\phi,t) = \theta_t(\phi) + \int_{r}^{r_t(\phi)} \frac{n_0 x_0 \, dr}{r\cos\phi \sqrt{n^2(r,t)r^2 - n_0^2 \dfrac{x_0^2}{\cos^2\phi}}}, \tag{7}$$

where $x_0 = r_0 \sin\theta \cos\phi$.

The screen is located at the distance z_1, the radial coordinate at the screen $r(z_1,\varphi)$ defines from equation $r\cos\theta(r,\varphi) = z_1$ and the coordinates of laser sheet at the screen are

$$x(z,\phi) = r(z,\phi)\sin\theta(r(z,\phi),\phi)\cos\phi, \tag{8}$$

$$y(z,\phi) = r(z,\phi)\sin\theta(r(z,\phi),\phi)\sin\phi. \tag{9}$$

At $z = z_0$ the laser sheet equation is: $x = x_0$. The shooting parameter ρ of the ray corresponding to the angle φ is equal $\rho = x_0/\cos\varphi$ and the trajectory of this ray is the function $r(\theta, \varphi)$. The radial coordinate of the ray at $z = z_0$ is $r_0(\varphi)$ and its direction defines by angle $\theta_0(\varphi)$.

The 2 or 3-dimensional experimental or calculated refraction images of spatially discrete SLB are called 2D *or* 3D-*refractograms*. The problem of LS propagation in media with radial variation of the temperature and refractive index is solved in [4]. Figure 6 shows the 2D-refractograms which typical by using of cylindrical SLB for visualization of the boundary layer near the heated metal ball in cold water [5].
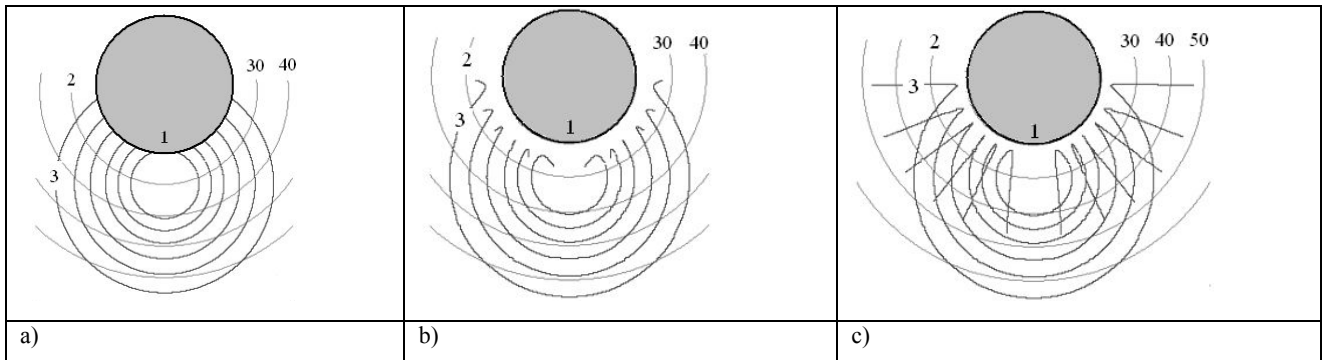

Fig. 6. Variation of the 2D refractograms of a cylindrical beam near a heated ball (*1* – ball, *2* – grid lines, *3* – beam projection on the screen): (*a*) $T = 90$ °C, $R = 20$ mm, $a = 2$ mm, $z = 100$ mm; (*b*) $T = 90$ °C, $R = 20$ mm, $a = 0.6$ mm, $z = 200$ mm; (*c*) $T = 90$ °C, $R = 20$ mm, $a = 0.5$ mm, $z = 200$ mm (a – boundary layer thickness)

2.3 Laser sheet propagation in dynamic plane two layered medium

To study the diffuse layer between two different liquids is necessary for many problems in chemistry and geophysics to be solved [3]. A schematic diagram of the experimental setup is presented in Fig. 7. LS 1 is passed through diffuse layer 2 confined in a cell, and the distortion that the beam suffers as a result of its refraction in the layer is observed on screen 3. The length of the cell is L, its breadth is B. The liquid interface is at a distance of x_s.
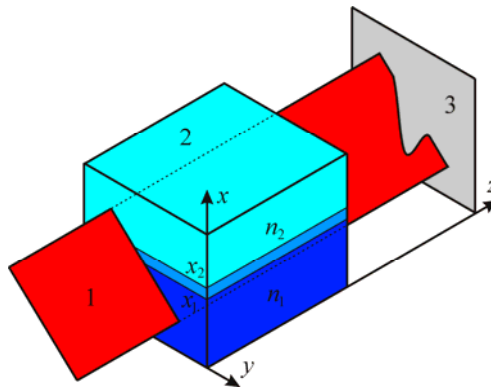

Fig. 7. Geometry of the problem: 1 – LS; 2 – plane two layered medium, 3 – screen

The ray trajectories in the diffuse layer were calculated as follows. The refractive index gradient in the diffuse layer may be described by formula (10) below that agrees well with the experimental relationship:

$$n(x,t) = n_1 - \frac{(n_1 - n_2)}{1 + \exp\left(-\frac{(x - x_s)}{h(t)}\right)} \tag{10}$$

where n_1 is the refractive index of the higher-density (bottom) liquid, n_2 is the refractive index of the lower-density (top) liquid, $h(t)$ is he characteristic half-breadth of the layer, and x_s is the position of the center of the layer.
The propagation of rays in the diffuse layer of two liquids is described by the following relation

$$z(x,t) = \int_x^{x_0} \frac{n(x_0)\sin(\theta_0)}{\sqrt{n^2(x,t) - n^2(x_0)\sin^2(\theta_0)}} \, dx, \qquad (11)$$

where θ_0 is the angle of entry of the ray into the layer, x_0 is the coordinate of the ray entrance point, $n(x)$ is the refractive index at the point x, and $n(x_0)$ is the refractive index at the point x_0

Figure 8 presents theoretical 2D refractograms for various refractive indices of the bottom liquid layer. The refractograms were calculated for conditions close to the experimental ones: the laser beam inclination angle $\alpha = 45°$, the refractive index n_1 of the bottom liquid layer varying over the range 1.335–1.356, the refractive index of the top liquid layer $n_2 = 1.332$, refractograms observed on the inner wall of the cell at a distance of $L = 300$ mm, the diffuse layer center $x_s = 50$ mm, and the layer half-breadth parameter $h = 1$ mm.
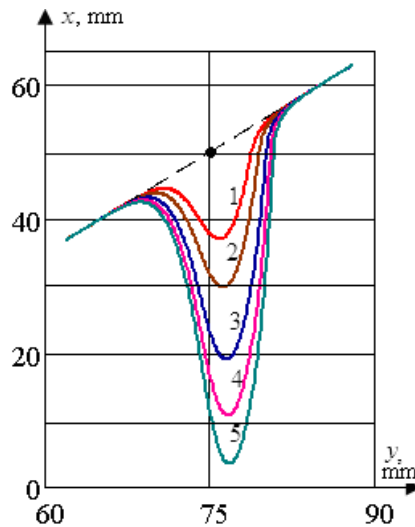

Fig.8. Theoretical 2D refractograms for various refractive indices of the bottom liquid layer

Figure 9 illustrates the formation of a refractogram with three laser sheets. The pertinent calculations were performed by formula (11) for the following law governing the variation of the refractive index in the diffusion layer:

$$n(x,y) = \frac{n_1 + n_2}{2} + \frac{n_1 - n_2}{2}\tan\left(\frac{x - x_s + a \cdot y}{h_0}\right), \qquad (12)$$

where $n_1 = 1.335$, $n_2 = 1.332$, $x_s = 20$ mm, $h_0 = 2.5$ mm, $a = 0.1$.
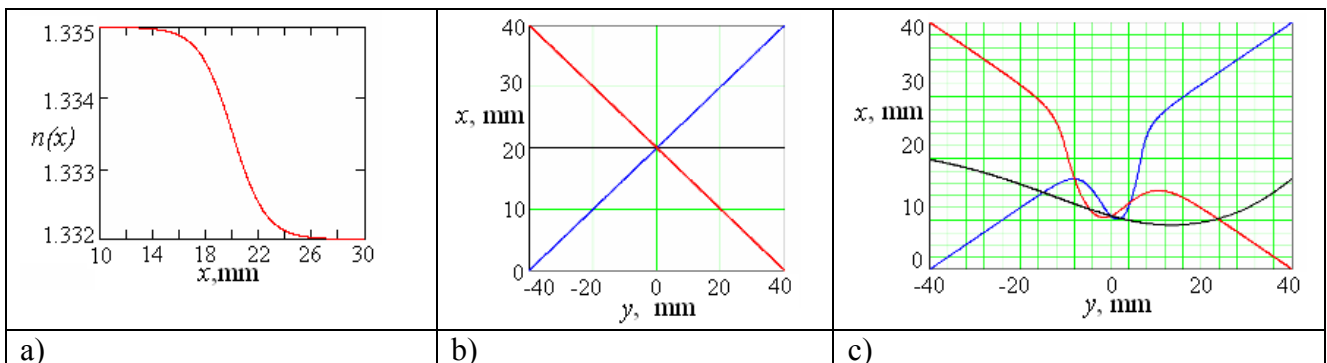

a)	b)	c)

Fig.9. The refractograms for three laser sheets: a) reftractive index distribution, b) laser sheets (black, red and blue lines) before cell at the time $t = 0$, c) refractograms (black, red and blue) for inclined diffuse layer (at angle 6°) for time $t > 0$.

3. EXPERIMENTAL REFRACTOGRAMS

3.1 Free laminar convection visualization near different bodies

Visualization by laser sheet. During the experiment different DOE were used for obtaining different SLB: thin laser beam, laser sheet (LS), cross-type, and concentric beams. The trace of thin LS image change on screen 5 (Fig.1) is shown in table 2. The LS passes under the bottom of different objects: parallelepiped with size of 38 x 27 mm^2 and the steel ball of 41.2 mm in diameter. These objects were heated up to T_r then placed in cold water to the depth 45-50 mm. The thickness of LS under the bottom of heated object, measured for the 1/e level, was 0.07 mm. In all cases it was smaller than boundary layer thickness, which was 1-3 mm.

From Fig.5,6 one can see, that initial LS, which is traced on the screen as a line, is deformed under the optical inhomogeneity of the liquid influence. This deformation depends from both the distance between LS and the object's surface and the time. LS deformations also severely depend on the shape of the heated object. After the object is cooling, LS returns to its initial form. The magnitude of deformation – time diagram allows to determine the cooling time of heated object or the heating time of the cooled one.

Table 2. Refractograms of a laser sheet (LS) passing close to heated bodies

No.	Objects and illumination conditions	Object shape and probing direction	Refractograms
1	Parallelepiped – LS passes beneath the bottom of the parallelepiped along its long side		
2	Cylinder – LS passes beneath the base of the cylinder placed vertically		
3	Thick-walled cylinder – LS passes beneath the base of the cylinder		
4	Ball – LS passes beneath the bottom point of the surface of the heated ball		
5	Right prism with an apex angle of 90° – LS passes along the hypotenuse of the base of the prism		

Visualization by conical beams. Refractograms for conical beams, under the ball surface in cold water are shown on Fig. 10. The analysis of several refractograms for different times allows to determine mechanisms of ball's surface cooling or heating[5].

Figure 10 presents experimental cylindrical SLR refractograms obtained for a boundary layer near a heated ball with a radius of $R = 25.4$ mm at a distance of $z = 156$ mm from its center: (*a*) initial beam; (*b*) surface temperature $T(R) = 65$ °C; (*c*) surface temperature $T(R) = 37$ °C.
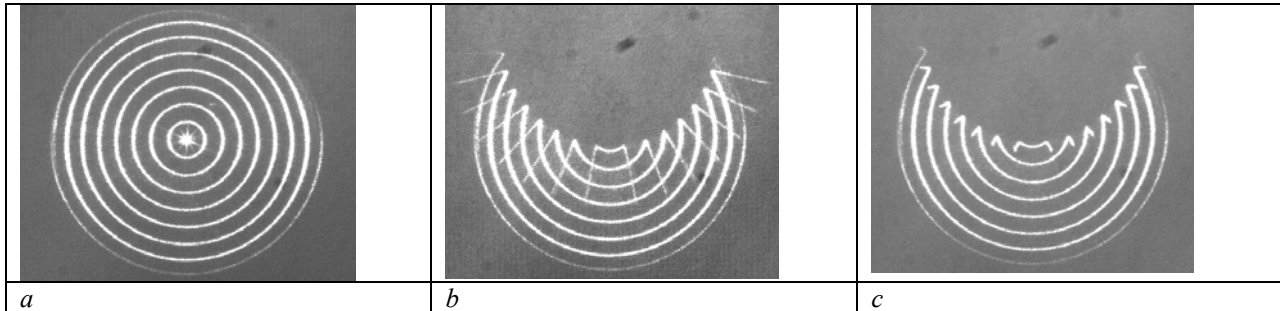

a   *b*   *c*

Fig. 10. Conical beams refractograms under the heated ball surface: *a* – initial conical beams, *b* – refraction image for $T(R)$=65ºC, *c* – refraction image for $T(R)$=37ºC

3.2. Visualization of dynamic plane two layered medium

Visualization of internal waves by a wide laser beam. The experiment was as follows. The wide beam 60 mm in diameter was obtained by means of an optical system from a solid-state laser 0.53 μm in radiation wavelength. A two-layer liquid was produced in a 1500 mm long cell. Presented in Fig. 11 are direct shadowgraphs showing bright strips that indicate the inclination of the wave front. It should be noted that a bright strip does not indicate the position of the center of the layer.
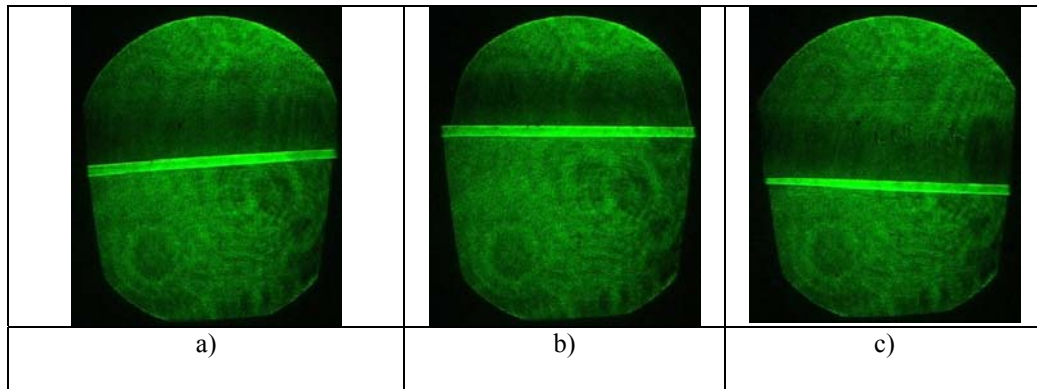

a)   b)   c)

Fig.11 Visualization of internal waves by a wide beam for different times: a) left side, b) top, c) right side

Visualization by two laser sheets. Used in the experiment were two 15 mW lasers: semiconductor operating at a wavelength of 0.650 μm and solid-state operating at a wavelength 0.532 μm. Such lasers radiation allows obtaining bright, high-contrast refractograms, capable of being well visualized on a screen in daylight. Laser sheets inclination angle was 90°.

Figure 12 presents a schematic diagram of the experimental setup for the visualization of internal waves in a two-layer liquid. It comprises two lasers, *1* and *4*, optical systems *2* and *5* for forming laser sheets *3* and *6*, semitransparent mirror *7*, cell *8* containing the two-layer liquid under study, liquid agitation generator *9*, screen *10*, CCD camera *11*, and personal computer *12*.
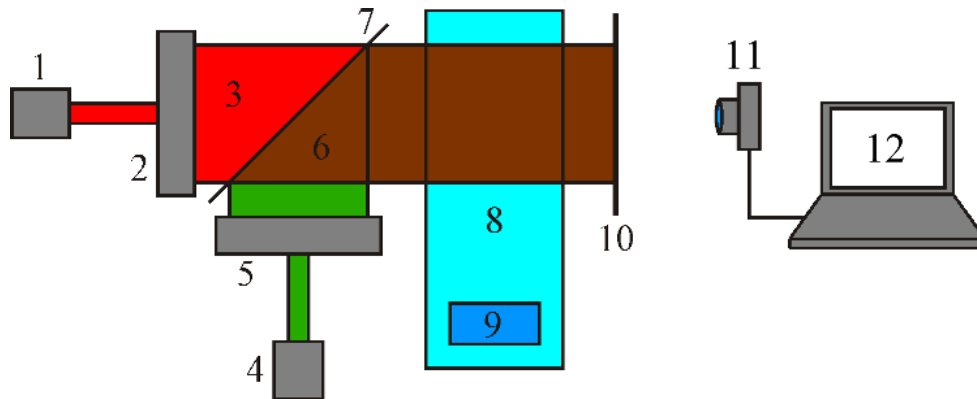
Fig. 12. Schematic diagram of the experimental setup (top view): *1* – laser (λ = 0.65 μm), *2* and *5* – optical systems for forming laser sheets *3* and *6*, *4* – laser (λ = 0.53 μm), *7* – semitransparent mirror, *8* – cell containing the two-layer liquid, *9* – liquid agitation generator, *10* – screen, *11* – CCD camera; *12* – personal computer

Figure 13 presents typical refractograms, illustrating the variation dynamics of the two-layer liquid.

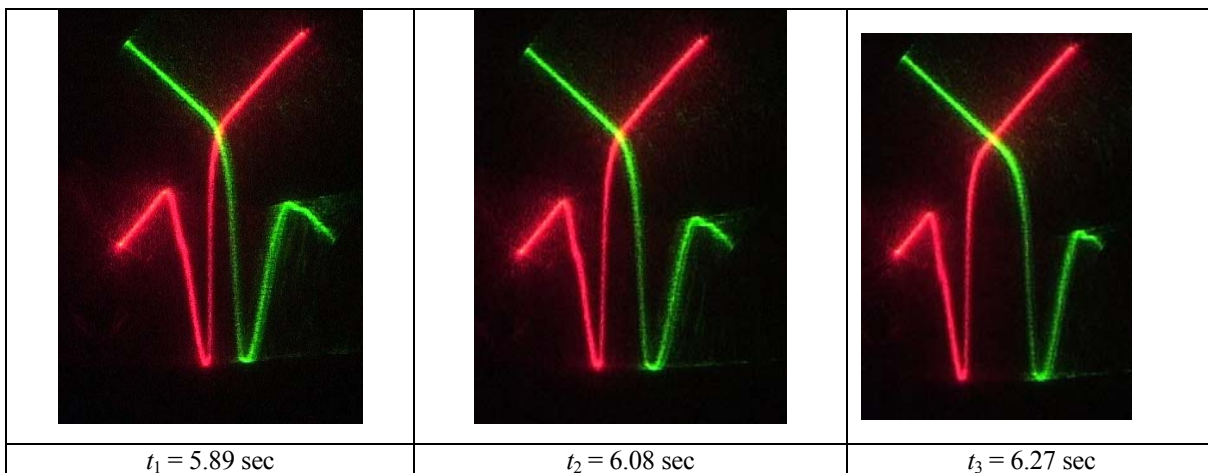| $t_1 = 5.89$ sec	$t_2 = 6.08$ sec	$t_3 = 6.27$ sec

Fig.13 Experimental 2D-refractograms laser sheets in dynamic two layer liquid for different times: $t_1 < t_2 < t_3$

4. COMPUTER PROCESSING OF REFRACTOGRAMS

Laser rerfractography is a technique providing not only for qualitative, but also for quantitative visualization of optically inhomogeneous flows. This end can be attained if one has at one's disposal a theoretical model of the process of interest, obtained by solving the pertinent thermophysical problem. Figure 14 illustrates the reconstruction of the temperature profile in a boundary layer next to a cooled ball 50.8 mm in diameter by comparison of an experimental refractogram (red dots) with its theoretical counterpart (solid curve).
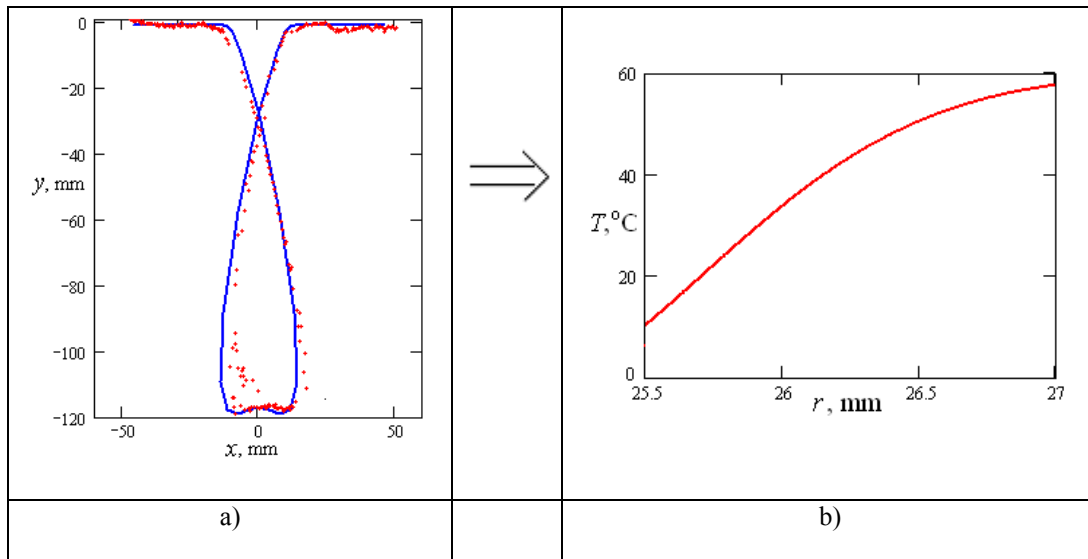
Fig. 14 Comparison between an experimental and theoretical refractograms: a) experimental refractogram – red dots, theoretical refractogram – blue line, b) the reconstructed temperature profile in boundary layer

Figure 15 shows comparison between an experimental refractogram and its theoretical countrparet and the reconstructed refractive index distribution profile in the diffuse layer.
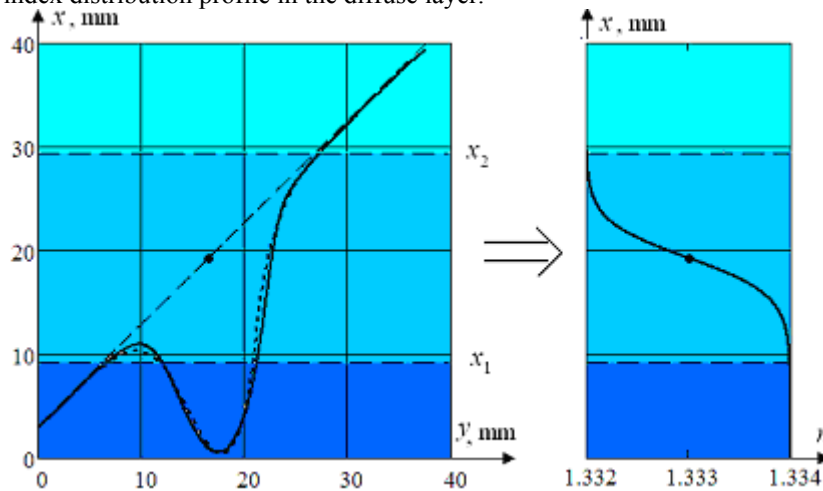

Fig. 15. Reconstruction of the refractive index distribution: (*a*) experimental refractogram (solid curve) and its theoretical model (dotted curve); (*b*) refractive index distribution profile.

Other applications of LAREF technique presented in the works [4,11,12].

CONCLUSION

✓   Modern stage of optically inhomogeneous   medium diagnostics refractive methods development is characterized by using of coherent light sources, new optical elements including DOE and refractive image computer processing.

✓   Rather high space coherence of laser beams produced with the help of DOE allows creating of structured laser beams adapted to the investigated flows.

✓   Laser refractography is the next step in refractive methods development and allows receiving of both 2D and 3D refractograms which are more vivid and informative.

✓   Laser refractography is oriented not only on inhomogeneity visualization, but also on getting quantitative information about optically inhomogeneous flows.

✓   Laser refractography can be used not only for stationary process diagnostics but also for fast nostationary process diagnostics, including investigation of heat processes in liquids, gas and plasma, free convection in liquids near heated and cold bodies, processes of different liquids mixing in chemical technology devices.

ACKNOWLEDGEMENTS

REFERENCES

[1] Settles G.S. *Schlieren and Shadowgraph Techniques*. Springer, 2001.

[2] Rinkevichius B.S. *Laser Diagnostics in Fluid Mechanics.* N-Y, Begell House, Inc., 1998

[3] Fomin N.A. *Speckle photography for fluid mechanics measurements.* Springer, Berlin, 1998

[4] Rinkevichyus B.S., Evtikhieva O.A., Raskovskaya I.L. *Laser refractography*. Springer. New York. 2011

[5]. Raskovskaya I.L., Rinkevichyus B.S., Tolkachev A.V. *Structured Beams in Laser Refractography Applications*. In books: *Laser Beams Theory. Properties and Applications*. Nova Science Publishers. Inc. New York, pp.399-414, 2011.

[6] Raskovskaya I.L., Rinkevichyus B.S., Tolkachev A.V. *Laser Refractography of Optical Heterogeneity Mediums.* Quantum Electronics., Vol.37, No.12, pp.1176-1180. 2007.

[7] Kravtsov U.A., Orlov U.I. *Geometrical optics of inhomogeneous medium*. Moscow, Nauka Press, 1980.

[8] Kuzmicheva M., Raskovskaya I.L. Computer visualization of the structured laser radiation refractograms *. Proc.* 15*th International Symposium on Flow Visualization.* June 25-27, Minsk, 2012

[9] Lapitski K.M., Raskovskaya I.L., Rinkevichyus B.S. Quantitative visualization of transparent spherical temperature layer. *Proc.* 12*th International Symposium on Flow Visualization*. September 10-14, Geottingen, paper 055, 2006.

[10]. Krikunov A.V., Raskovskaya I.L., Rinkevichyus B.S. *Refraction of an Astigmatic Laser Beam in a Transition Layer of Stratified Liquid*. Optics and Spectroscopy.Vol.111, No.6, pp. 956-981, 2011

[11] Raskovskaya I.L. *Laser beam propagation in the medium with acoustical wave.* Radiotekhnika i elektronika. Vol.49, No.11, pp.1382-1389, 2004.

[12] Yesin M.V., Evtikhieva O.A., Orlov S.V., Rinkevichius B.S., Tolkachev A.V. Laser refractometral method for visualization of liquid mixing in twisted flows. CD Rom Proceedings. 10-*th International Symposium on Flow Visualization*. (Kyoto. August 26-29. 2002). Paper No. F037. 2002.